Original

Stark, A.; Schimansky, F.-P.; Clemens, H.:

Texture Formation during Hot-Deformation of High-Nb Containing Gamma-TiAl Based Alloys

In: Solid State Phenomena, Texture and Anisotropy of Polycrystals III (2010)
Trans Tech Publications

DOI: 10.4028/www.scientific.net/SSP.160.301

Solid State Phenomena Vol. 160 (2010) pp 301-306
© (2010) Trans Tech Publications, Switzerland
doi:10.4028/www.scientific.net/SSP.160.301

Texture Formation during Hot-Deformation of High-Nb Containing γ-TiAl Based Alloys

A. Stark[1,2,a], F.-P. Schimansky[2,b] and H. Clemens[3,c]

[1]Institute of Materials Science and Technology, Hamburg University of Technology, Eißendorfer Str. 42, D-21073 Hamburg, Germany

[2]Institute of Materials Research, GKSS Research Centre, Max-Planck-Str. 1, D-21502 Geesthacht, Germany

[3]Department of Physical Metallurgy and Materials Testing, Montanuniversität Leoben, Franz-Josef-Str. 18, A-8700 Leoben, Austria

[a]Andreas.Stark@gkss.de, [b]Frank-Peter.Schimansky@gkss.de, [c]Helmut.Clemens@unileoben.ac.at

Keywords: TiAl, Forging, Texture, Microstructure, Intermetallics

Abstract. In this study texture and microstructure formation in high-Nb containing TiAl alloys during lab-scale compression experiments and "near conventional" forging on an industrial scale are investigated. The deformation temperatures range from 700 °C up to temperatures close to the α-transus temperature (T_α = 1295 °C). Depending on the deformation conditions, the texture of the tetragonal γ-TiAl phase is formed by pure deformation components, components related to dynamic recrystallization, or transformation components. This changing corresponds with microstructural observations. The hexagonal phases α_2-Ti_3Al and α-Ti(Al) show a similar texture as it is known for Ti and Ti-base alloys after compressive deformation at elevated temperatures. In contrast to the γ texture, no significant change of the α/α_2 texture was observed in the investigated temperature range. In the alloy with a composition of Ti-45Al-10Nb (in at.%) even deformation textures of ternary intermetallic phases, as the hexagonal ω_o-Ti_4Al_3Nb and the cubic β_o-TiAl(Nb) phase, respectively, were measured and analyzed.

Introduction

Intermetallic γ-TiAl based alloys are attractive candidates for high-temperature structural applications in industrial and in aviation gas turbines due to their high strength, low density and good oxidation resistance [1]. In order to extend their service range to higher temperatures research activities have been focused on high-Nb bearing TiAl alloys. These so-called 3rd generation alloys exhibit a significant increase in strength combined with improved creep properties [2-4]. Several thermo-mechanical processing routes, such as hot rolling, extrusion and forging, have been established for conventional γ-TiAl based alloys. However, up to now there is no well-established wrought processing route, which guarantees an economic and continuous supply of turbine components made of γ-TiAl. In order to increase the economic feasibility a "near conventional" forging of γ-TiAl based alloys has been developed [5].

Thermo-mechanical processing of γ-TiAl based alloys often results in anisotropic mechanical behavior due to the formation of crystallographic textures and several papers dealing with texture analysis in γ-TiAl alloys are published in the last years [6-9]. Many of them are focused on the texture formation of the tetragonal γ-TiAl phase. However, γ-TiAl based alloys are multiphase alloys and especially during hot working α-Ti(Al) is often the predominant phase. Moreover, Nb is known as a β-Ti(Al) stabilizing element, thus γ-TiAl based alloys with high Nb contents show an increased fraction of β phase which might transform to ω_o phase at lower temperatures [10,11].

In this paper, the textures of γ, α/α2 and, if present, β_o and ω_o phases, after hot compressive deformation are analyzed and their possible interaction during formation is discussed. The results

obtained during "near conventional" forging on an industrial scale are compared with those derived from laboratory experiments.

Experimental

High-Nb bearing γ-TiAl alloys with a composition of Ti-45Al-xNb (in at.%), x = 5, 7.5, and 10, were used for hot-compression experiments on a laboratory scale. The results are compared with texture measurements of industrially forged material with a composition of Ti-45Al-5Nb. In order to start with texture-free and microstructurally as well as chemically homogeneous material hot-isostatically pressed (HIP) powder compacts were used for the lab-scale experiments as well as for the industrial processing. The powder was produced in the PIGA-facility (Plasma Melting Induction Guiding Gas Atomization) at the GKSS Research Centre. Powder of the size fraction < 180 µm was filled in Ti cans, which then were degassed and subsequently HIPed at 200 MPa for 2 h at 1250 °C.

The lab-scale uniaxial compression tests were performed in air in the range of 700 °C to 1100 °C, with constant true strain rates of $5x10^{-4}$ s^{-1}, $5x10^{-3}$ s^{-1}, and $5x10^{-2}$ s^{-1}, respectively. Cylindrical specimens of 10 mm in diameter and 15 mm in height were heated up to test temperature in about 15 min, then they were compressed to a total strain of $\varepsilon = -1$ (63% reduction in height) followed by oil quenching to avoid recrystallization effects due to residual heat. The industrial forging was conducted at 1200 °C, 1270 °C, and close to T_α. Specimens of 41 mm in diameter and 44 mm in height were forged to an overall logarithmic strain of approximately $\varepsilon = -0.7$ (50% reduction in height) followed by air cooling. The total contact time between the TiAl billet and the dies lasts up to 60 seconds depending on die speed and total stroke. Because hot-forging is performed on a conventional 1000 t hydraulic press without any special isothermal forging equipment, the forging process used in this study is considered as "near conventional" [5].

Microstructure observation was made by light-optical microscopy (LOM) using polarized light and scanning electron microscopy (SEM) in back-scattered electron (BSE) mode. The volume fractions of the different phases within the samples were estimated by Rietveld analysis of X-ray diffraction (XRD) measurements as well as by quantitative metallographic evaluation conducted on LOM images derived from color-etched samples and SEM images taken in BSE mode.

Texture measurements have been performed by X-ray diffraction (XRD) in reflection geometry with filtered CuKα radiation using a texture goniometer with Eulerian cradle from Bruker AXS. Due to the parallel beam optic, a very low background level and a high peak resolution even at high pole distance angles (χ) are achieved. This facilitates the separate measuring of the narrow {002} and {200} γ reflections as well as of the weak α_2 reflections. Pole figures were measured up to a χ angle of 85° and subsequently corrected for background and intensity loss. The orientation distribution function (ODF) of the γ phase was calculated by using the series expansion method [12] up to an order of 22. The ODF of the α/α_2 phase and the ternary phases in Ti-45Al-10Nb was calculated employing the WIMV algorithm of the BEARTEX Berkeley Texture Package [13]. Subsequently complete and inverse pole figures were recalculated from the ODF.

Additionally, the texture formation during compressive deformation in γ-TiAl was simulated. The single-crystal yield surface model of γ-TiAl according to Mecking et al. [14] is applied to polycrystal deformation with the help of the Los Alamos polycrystal plasticity Code. The input parameters for the simulation are the ratios of the critical resolved sheer stresses (CRSS) for ordinary dislocation slip (τ_o), super dislocation slip (τ_s), and for mechanical twinning (τ_t), as described in detail in [15].

Results and Discussion

Microstructure and Phase Composition. The HIPed powder compacts show a fine-grained equiaxed duplex microstructure (Fig. 1a). The grain sizes are in the range of 10 to 20 µm. In the alloy with 10 at.% Nb the grain size is slightly larger and the fraction of lamellar ($\alpha_2+\gamma$) colonies is

significantly lower. The XRD pattern of Ti-45Al-5Nb and Ti-45Al-7.5Nb show only peaks of α_2 and γ phase, whereas in the alloy with 10 at.% Nb a third phase can clearly be identified as ordered ω phase, ω_o-Ti_4Al_3Nb, with $B8_2$ structure [10,11]. The phase fractions amount to approximately 75 vol.% γ and 25 vol.% α_2 for the alloys with 5 and 7.5 at.% Nb. Ti-45Al-10Nb consists of about 80 vol.% γ, 10 vol.% α_2 and 10 vol.% ω_o.

After compression at 700 °C and 800 °C the microstructure is mainly affected by pure deformation. The α_2 and γ grains are elongated perpendicular to the compression direction (Fig. 1b) and show a significant aspect ratio. Starting at 800 °C, and clearly observable at 900 °C (Fig. 1c), the deformed large grains are surrounded by extremely fine-grained areas of dynamically recrystallized (DRX) α_2 and γ phase. With increasing deformation temperature the proportion of the DRX areas as well as their grain size increases. At 1100 °C the microstructure mainly consists of DRX grains (Fig. 1d). Bended grain boundaries indicate a bulging mechanism during DRX. Many small grains can be detected leading to a relatively inhomogeneous grain size distribution and the aspect ratio is mostly vanished. The specimens forged at 1200 °C and 1270 °C (Fig. 2a) also exhibit a fine-grained microstructure due to a high degree of DRX. The grain size of DRX γ-TiAl rises and the volume fraction of γ phase decreases with increasing forging temperatures. In the specimen forged close to T_α (Fig. 2b) only a small amount of γ grains, about 5 vol.%, exists between large former α grains. The former α grains show a distinct aspect ratio. During cooling they transformed to lamellar (α_2+γ) colonies.

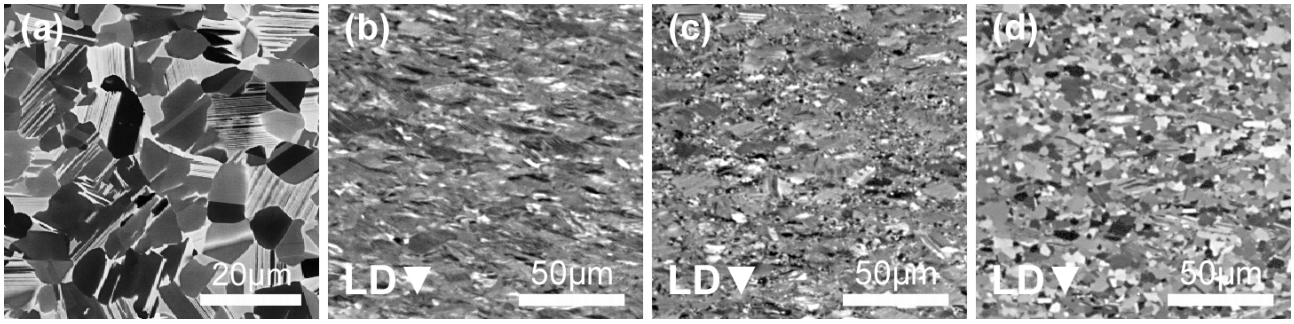

Fig. 1: Typical microstructures (Ti-45Al-5Nb): (a) HIPed starting material (REM image in BSE mode), (b-d) after lab-scale compression at (b) 700 °C, (c) 900 °C, and (d) 1100 °C (LOM images, polarized light; LD = load direction).

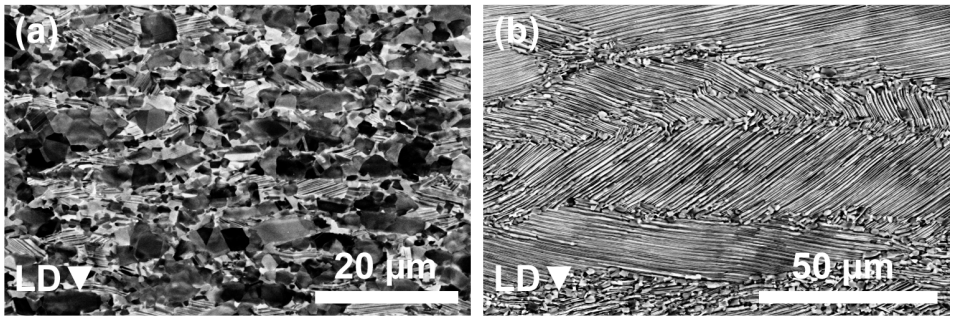

Fig. 2: Microstructure of Ti-45Al-5Nb after industrial forging at (a) 1270 °C, and (b) close to T_α. REM images in BSE mode.

Texture Formation in the γ-TiAl Phase. After deformation at 700 °C, the γ-TiAl phase shows three characteristic texture components when described by inverse pole figures in load direction (Fig. 3a). One orientation maximum is formed at <110> and a second at about <302>. The stable orientations in fcc metals after compressive deformation are located at <110> and <101> which are symmetrically equivalent positions in the cubic system. Due to the tetragonal $L1_0$ structure of γ-TiAl the ideal cubic maximum at <101> is shifted towards <100> resulting in <302>. The third characteristic component is a metastable maximum at about <411> which is connected with <110> and <302> by a band showing a high orientation density.

Computer simulations of the deformation texture (Fig. 3e, f) agree well with the measured textures after compression tests at 700 °C. The orientation flow maps of γ-TiAl, calculated with

CRSS ratios τ_o/τ_s = 0.8 and τ_t/τ_s = 0.2 show an orientation flow towards <110> and <302>. At <411> the direction of the orientation rotation changes and their flow becomes slower. This leads to the metastable orientation maximum around <411>. At higher degrees of deformation, mechanical twinning, represented by long arrows in Fig. 3f, produces an additional accumulation of orientation density around <110>. This means that the texture measured after compression at 700 °C is exclusively generated by activation of slip systems and mechanical twinning and, therefore, represents a pure deformation texture.

The pure deformation texture diminishes with increasing deformation temperature (Fig. 3b). The metastable maximum around <411> vanishes between 800 °C to 900 °C. The maximum around <110> becomes continuously weaker and disappears completely at 1100 °C. Only the <302> deformation texture component stays stable even at this temperature. Simultaneously a new orientation maximum around <100> is formed with increasing deformation temperature. Thus, the <100> position is the preferred orientation generated during DRX [16]. At 1100 °C the texture is mainly affected by DRX (Fig. 3c). The inverse pole figure shows a broad band of orientation density between <100> and <101>.

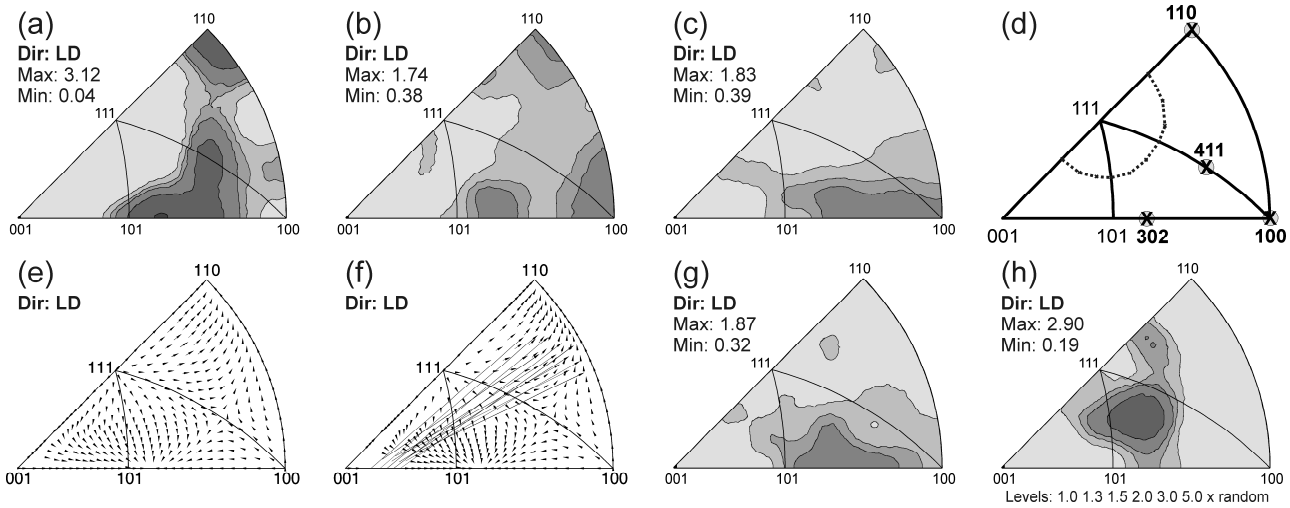

Fig. 3: Inverse pole figures in load direction of γ-TiAl. (a-c) After lab-scale compression of Ti-45Al-7.5Nb at (a) 700 °C, (b) 900 °C, and (c) 1100 °C. (d) Sketch with the positions of characteristic components. (e, f) Simulation of the deformation texture at (e) ε = 0.05, and (f) ε = 0.15. (g, h) After industrial forging of Ti-45Al-5Nb at (a) 1270 °C, and (b) close to T_α.

During DRX new nuclei are generated continuously. Obviously, those nucleated at orientations around <100> have the best growing conditions. They grow at the expense of adjoining grains, especially at the expense of grains orientated around <110>, which are mainly formed by mechanical twinning. The twins act as starting points for recrystallization [17] and the grains are consumed in the course of the recrystallization process. Due to the continuing compressive deformation, the new grains formed by DRX rotate towards <302>. The process of nucleation, growth and rotation takes continuously place during DRX. This provides an obvious explanation for the formation of the orientation band between <100> and <101> and the vanishing of pure deformation texture components.

Also after forging at 1200 °C and 1270 °C, γ-TiAl shows a typical DRX texture (Fig. 3g), similar to that present after compression at 1100 °C. This texture is in consistence with the observed DRX microstructure shown in Fig. 2a. However, the γ texture after forging close to T_α (Fig. 3h) exhibits components that can be explained neither by deformation nor by DRX. In this specimen, the most part of γ has been formed by the transformation of α to γ during cooling after the deformation. Thus, γ shows a distinct transformation texture that does conserve the α deformation texture, as discussed later on (Fig. 4d, e).

Textures of α_2-Ti_3Al and α-Ti(Al). The deformation texture of α_2-Ti_3Al was measured after lab-scale forging experiments ranging from 800 °C to 1100 °C. The texture is formed by a tilted <0001> basal fiber with a tilt angle of about 20° between load direction and fiber axis. A typical inverse pole figure in load direction is shown in Fig 4a. Tilted basal fiber textures with a tilt angle of about 20° are also reported for α-Ti and other hcp metals with a c/a-ratio < 1.63 after compressive deformation [18]. The α-Ti(Al) deformation texture in the specimens forged between 1200 °C and close to T_α is formed by a tilted basal fiber too. However, after forging close to T_α the texture becomes sharper and stronger because of the almost exclusive deformation of α phase at this temperature (Fig 4b). In contrast to the γ texture, the α/α_2 texture does not change with increasing temperature. Although the forging experiments took place at temperatures below and above the α_2 to α transition no difference is seen between α_2 and α textures obtained after compression. That means that during uniaxial compression at elevated temperatures the same slip systems are activated in α_2-Ti_3Al and α-Ti(Al), making the ordering of α_2-Ti_3Al negligible.

A crystallographic relationship of the α/α_2 deformation texture was observed neither to the γ deformation texture nor to the γ texture formed by DRX. This indicates that the textures of both phases are generated independently of each other during uniaxial compression. A γ texture component according to the Blackburn relationship, $\{111\}\gamma \parallel \{0001\}\alpha_2$ and $<1\bar{1}0>\gamma \parallel <11\bar{2}0>\alpha_2$, should form a ring of 20° distance around the <111> orientation as shown in sketch Fig. 3d. Exactly this component can be observed in the specimen forged at close to T_α (Fig. 3h). Moreover, this correlation is illustrated by the central part of the recalculated pole figures of {0001}α and {111}γ (Fig. 4c, d). The lower intensity and the additional orientation density at the rim of the recalculated {111}γ pole figure is due to the four <111> axes of the tetragonal system which are related only to a single <0001> axis of the hexagonal system.

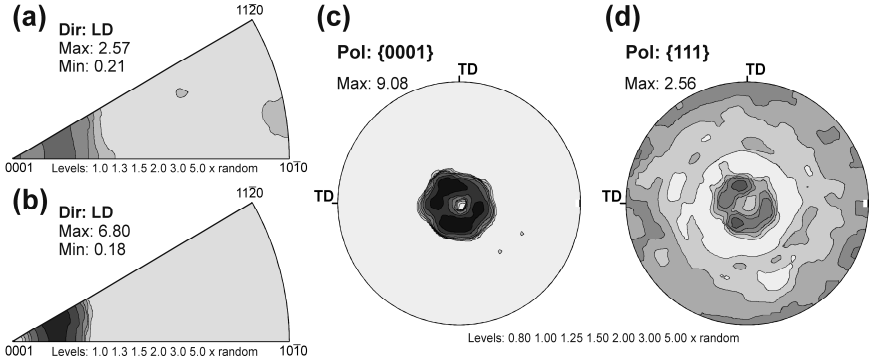

Fig. 4: Inverse pole figures of (a) α_2 after forging at 900 °C, and (b) α after forging close to T_α. Correlation of (c) the α deformation texture and (d) the γ transformation texture after forging close to T_α .

Textures of ω_o and β_o in Ti-45Al-10Nb. In Ti-45Al-10Nb the amount of Nb-rich ternary intermetallic phases is high enough for measuring their deformation textures too. At temperatures slightly above 900 °C the ordered ω_o-Ti_4Al_3Nb phase with a hexagonal $B8_2$ structure transforms to ordered β_o-TiAl(Nb) phase with cubic B2 structure [11]. After deformation at 800 °C the $\{11\bar{2}0\}$, $\{10\bar{1}2\}$, $\{20\bar{2}2\}$, and $\{21\bar{3}2\}$ pole figures of the ω_o phase could be measured. The calculated texture results in an ideal <0001> basal fiber (Fig. 5a) which is a typical compression texture component in various hexagonal materials. The distinct texture formation indicates plastic deformation by dislocation slip in ω_o at elevated temperatures. In spite of its complex hexagonal structure, ω_o does not behave brittle during forging as it is assumed at lower temperatures [19].

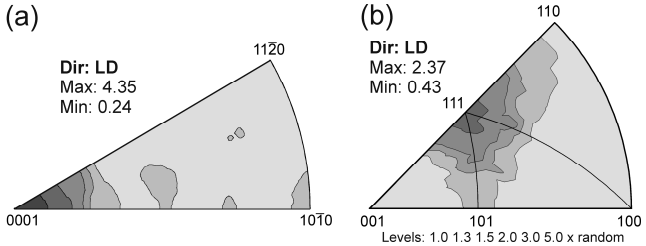

Fig. 5: Deformation textures of ternary phases in Ti-45Al-10Nb. (a) ω_o-Ti_4Al_3Nb after forging at 800 °C, and (b) β_o-TiAl(Nb) after forging at 1000 °C.

In case of compression tests conducted above 800 °C, {110} and {002} pole figures of the cubic β_o phase were measured. The β_o texture is formed by a pure <111> fiber as shown in Fig. 5b. This orientation is known as a stable orientation of bcc metals during uniaxial compressive deformation. The B2 structure of ordered β_o is closely related to the bcc structure of the disordered β phase. Thus, similar slip systems should be activated in both phases producing the same deformation textures.

References

[1] H. Kestler and H. Clemens, in: *Titanium and Titanium Alloys*, edited by C. Leyens and M. Peters, Wiley-VCH, Weinheim, Germany (2003), p. 351

[2] F. Appel, M. Oehring, J. D. H. Paul and U. Lorenz, in: *Structural Intermetallics 2001*, edited by K. Hemker, D. Dimiduk, H. Clemens, R. Darolia, H. Inui, J. Larsen, V. Sikka, M. Thomas and J. Whittenberger, TMS, Warrendale, PA, USA (2001), p. 63

[3] S. Bystrzanowski, A. Bartels, H. Clemens, R. Gerling, F.-P. Schimansky, G. Dehm and H. Kestler: Intermetallics Vol. 13 (2005), p. 515

[4] R. Gerling, F.-P. Schimansky, A. Stark, A. Bartels, H. Kestler, L. Cha, C. Scheu and H. Clemens: Intermetallics Vol. 16 (2008), p. 689

[5] S. Kremmer, H. F. Chladil, H. Clemens and A. Otto, in: *Ti-2007 Science and Technology*, edited by M. Niinomi, S. Akiyama, M. Hagiwari, M. Ikeda, K. Maruyama, The Japan Institute of Technology, Japan, (2008), p. 989.

[6] W. Skrotzki, R. Tamm, H. G. Brokmeier, M. Oehring, F. Appel and H. Clemens: Materials Science Forum Vol. 408-412 (2002), p. 1777

[7] H. Brokmeier, M. Oehring, U. Lorenz, H. Clemens and F. Appel: Metallurgical and Materials Transactions A Vol. 35 (2004), p. 3563

[8] A. Stark, A. Bartels, R. Gerling, F.-P. Schimansky and H. Clemens: Advanced Engineering Materials Vol. 8 (2006), p. 1087

[9] A. Stark, A. Bartels, H. Clemens, S. Kremmer, F.-P. Schimansky and R. Gerling: Advanced Engineering Materials (2009), *accepted for print*.

[10] L. Bendersky, W. Boettinger, B. Burton, F. Biancaniello and C. Shoemaker: Acta Metallurgica et Materialia Vol. 38 (1990), p. 931

[11] A. Stark, A. Bartels, H. Clemens and F.-P. Schimansky: Advanced Engineering Materials Vol. 10 (2008), p. 929

[12] M. Dahms and H. J. Bunge: Journal of Applied Crystallography Vol. 22 (1989), p. 439

[13] H. Wenk, S. Matthies, J. Donovan and D. Chateigner: Journal of Applied Crystallography Vol. 31 (1998), p. 262

[14] H. Mecking, C. Hartig and U. Kocks: Acta Materialia Vol. 44 (1996), p. 1309

[15] W. Schillinger, A. Bartels, R. Gerling, F.-P. Schimansky and H. Clemens: Intermetallics Vol. 14 (2006), p. 336

[16] A. Bartels and W. Schillinger: Intermetallics Vol. 9 (2001), p. 883

[17] F. Appel and R. Wagner: Materials Science and Engineering R Vol. 22 (1998), p. 187

[18] G. Wassermann and J. Grewen: *Texturen metallischer Werkstoffe*. Springer, Berlin, (1962).

[19] M. A. Morris and Y. G. Li: in *Gamma Titanium Aluminides*, edited by Y.-W. Kim, R. Wagner and M. Yamaguchi, TMS, Warrendale, PA, USA (1995), p. 353